Computers and Concrete, *Vol. 22, No. 3 (2018) 269-278*
DOI: https://doi.org/10.12989/cac.2018.22.3.269

Partial sectional confinement in a quasi-encased steel-concrete composite beam

Amir Masoud Hassanzadeh[a] and Mehdi Dehestani[*]

Faculty of Civil Engineering, Babol Noshirvani University of Technology, Babol, Iran

(Received January 31, 2017, Revised July 24, 2018, Accepted August 3, 2018)

Abstract. In the recent decades, the application of composite materials, due to their desirable properties, has increased dramatically. In the present study, a quasi-encased trapezoidal section composite steel beam encased with concrete is thoroughly examined. Calculation of the load bearing capacity is carried out by finite element modeling of concrete and FRP beams with trapezoidal section under the effect of controlled displacement loading. The results are then validated comparing to the existing experimental results obtained from similar studies. Further on, the materials are changed to steel and concrete, and the section is de-signed in such a way that both concrete and steel reach a high percent-age of their load bearing capacity. In the last step, the parameters affecting the bending capacity and the behavior of the semi-confined composite beam are investigated. Results revealed that the beam diagonal web thickness plays the most effective role in load bearing capacity amongst other studied parameters. Furthermore, by analyzing the results on the effect of different parameters, an optimal model for primary beam section is presented, which exhibits a greater load bearing capacity compared to the initial design with the same amount of materials used for both sections.

Keywords: composite structures; partial confinement; finite element method; boundary conditions

1. Introduction

Until a few decades ago, the construction of tall buildings was almost limited to steel and concrete structures, while either of them had their own structural and technological problems. The time and expenses required for beam steel reinforcement and framing, and the excessively high dead weight of the system, particularly in the presence of shear walls, are the two fundamental problems in concrete structures.

On the other hand, in metal structures because most column designs are buckled and lean, these structures become more expensive than their concrete counterparts, and in addition to that, the wages paid for building such structures are higher because of the difficulty of work at height and the necessity of high accuracy in the building and installation of metal frames, particularly concerning columns. Given these factors and some structural and technological issues, in the 1980s, the idea of composite structures for the optimal use of materials has been suggested in which concrete and steel are mixed in a new way. In composite structures, due to the higher compressive strength of concrete compared to its tensile strength, the use of concrete under pressure, results in the best expected behavior of concrete and also given the high tensile strength of steel, the use of steel as a buckling component, results in the most appropriate steel behavior in a structure. The optimal use of materials, results in reducing structure weight and construction costs, and with reduced structure weight, the force exerted on the foundation is reduced and as a result, less cross section and thickness will be resulted for the foundation. Actually, the purpose of the simultaneous use of materials is to increase efficiency while maintaining executive simplicity in construction. Because of the economic benefits and adequate structural behavior of composite steel-concrete beams, they have been widely used in past decades. Many research papers related to composite steel and concrete plate girders, such as Slutter and Driscoll (1965), Heins and Fan (1976), Manfredi *et al*. (1999), Ayoub and Filippou (2000), Thevendran *et al*. (2000), or to composite steel and concrete box girders, such as Mattock and Fountain (1967), Schelling *et al*. (1992), Sennah and Kennedy (1999), Nakamura (2002) and Sennah *et al*. (2004) have been published. Great research results have been obtained for understanding the structural behavior of composite steel-concrete beams.

The behavior of hybrid girders subjected to patch loading was investigated by Chacon *et al*. (2013) for the case in which the plates that assembled the girders were transversally stiffened. For hybrid girders that were longitudinally stiffened, scant work is available. A numerical database of 255 simulations on longitudinally stiffened steel girders which were subjected to patch loading developed by the authors was also included in the study. To assess the resistance of longitudinally stiffened hybrid steel plate girders subjected to patch loading, the computed results are illustrated.

With the use of non-linear finite element analyses, the behavior of transversely stiffened plate girders in bending

∗Corresponding author, Associate Professor
E-mail: dehestani@nit.ac.ir
[a]Graduate Student
E-mail: a.m.hsnz@stu.nit.ac.ir

http://www.techno-press.org/?journal=cac&subpage=8 ISSN: 1598-8198 (Print), 1598-818X (Online)

and shear were investigated by Hendy and Chris (2008). In the study, slender symmetrical steel girders with and without axial force were considered. Post-buckling behavior of webs from finite element analysis (FEA) and other theories was examined by the paper.

Some tests were performed by Chapman and Balakrishnan (1964) on seventeen simply supported straight composite beams. The beams were tested in terms of failure under static concentrated and distributed loading, which was applied on the axis of the beam. Within the range the number of shear studs varied, the effect of slip on elastic and ultimate load behavior seen. In 1968, in order to take into account the inelasticity of steel, concrete and shear connector, Yam and Chapman (1986) proposed a numerical method of analysis. This method of analysis was used to investigate the effects of cross-sectional properties, span, strength and stiffness, connector distribution type of loading and strain hardening on the beam-slab interaction and ultimate load behavior.

A curved I-girder subjected to a combination of concentrated loads, and torsional moments underwent laboratory tests by Heins and Spates (1970). Their model was embedded in concrete blocks to provide a fixed support and was loaded within the elastic range.

To solve the equilibrium equations of a single curved I-girder subjected to bending and torsional moments in both elastic and inelastic ranges, Fukumoto and Nishida (1981) used the transfer matrix method. The behavior of curved flexural members under large torsional deformation was also investigated by them. Moreover, six simply supported curved I-girders of ordinary sizes were tested to failure under a concentrated load applied at the midspan. For all fabricated curved beam specimens with “span-length” to “radius of curvature” ratio ranging from 0.008 to 0.08, longitudinal residual stresses and initial out-of straightness were measured. Some tests performed by Nakai and Yoo (1988) on 27 models, offered some explanations on the effect of local buckling on the strength of bridge girders curved in the plan. Pure bending moment was applied to these model girders. An analytical method for evaluating the lateral buckling strength of curved I-girders have been developed in accordance with the second-order buckling analysis based on these experimental studies. Some tests on two sets of I-beams, one set comprising rolled sections and the other comprising built-up sections have been carried out by Shanmugam *et al*. (2002). They investigated the behavior and the ultimate load of steel plate girders with centrally located rectangular or circular web openings. The study was performed with the use of a finite element package called ABAQUS. The results of the finite element analysis have been verified using the experimental results of other researchers. In the study parameters such as the effect of web plate slenderness, flange stiffness and opening shape and size of ultimate load of such girders were included. The finite element analysis results were drawn as load-deflection relationship curves, which showed good agreement between the finite element and the experimental results. From the study, it was concluded that the response of the slender plate girder was significantly affected by the imperfections of the plate girders.

An automatic design procedure for obtaining the minimum weight design for non-uniform stiffened steel plate girders has been offered by Alghamdi (2003). It was not required by the direct search procedure to evaluate the design gradients, and the search for minimum weight design is done according to ASD or LRFD design specifications of the AISC (1994).

Practical and efficient reliability-based optimization approach to the design of both unstiffened and stiffened composite hybrid plate girders for high-way bridges had been presented by Hendawi and Frangopol (1994). The steel weight of the built-up plate girder should be minimized, and all constraints specified in the AASHTO (1983) bridge code were considered in the optimization process. To find the rates of change of the optimum solution with respect to changes in problem pre-assigned parameters, some sensitivity analyses were also done.

An analytical method was offered by Darehshouri *et al*. (2013) to determine the ultimate shear capacity of composite plate girders containing web openings. In their method, the effects of composite action between the concrete deck and steel part of the girder and the presence of openings in the webs have been considered. The method accuracy was evaluated by making a comparison between the predicted values and the corresponding experimental results. Furthermore, the effects of web openings on ultimate shear capacity of composite girders were investigated. A number of composite plate girders containing centrally square and circular opening were tested up to the level of failure. The results acquired for circular, square and rectangular openings revealed that the ultimate shear capacity was significantly affected by the size of the openings, i.e., there was nearly a 30% drop when the depth of openings was increased to half the web depth of the girder. Openings that had larger depth displayed larger drop in shear resistance. It was concluded that the suggested method was able to predict the ultimate shear capacity of composite plate girders, where the depth of web opening had a greater influence on the shear capacity of these girders.

Kyung *et al*. (2011) visually inspected the load test and the structural analysis to discover the causes of the cracks of the steel plate girder railway bridge with a 65-year service history. The study suggested some suitable retrofitting methods for the fatigue cracks at welded joint. The validity of the retrofitting methods of fatigue stress was verified based on some field test results. It was discovered that the sample bridge exceeded the allowable fatigue stress range, so it needs early maintenance and management because the fatigue crack is progressing fast.

Lee *et al*. (2011) evaluated the flexural ductility of the negative moment region of I-girder which had high-strength steel in which the yield stress of the steel is 680MPa based on the results of finite element analysis and experiment. A method to improve the flexural ductility of I-girder with high-strength steel by an unequal installation of cross beam and an optimal position of cross beam was suggested in the study. Also, based on the experimental results, the effects of the unequal installation of cross beam on the flexural ductility were discussed. It was concluded that the flexural ductility of the I-girder is highly reduced because of the increase in elastic deformation and also due to the decrease in the plastic deformation ability of the material when the yield strength increases.

Baskar *et al*. (2002) conducted a nonlinear analysis using finite element modeling for the prediction of the ultimate load behavior of steel–concrete composite plate girders under negative bending and shear loading. The results of the nonlinear analysis have been verified with one steel plate girder and four composite plate girders, which were tested to failure by other researchers. The conclusion was that the modeling of the deck slab using shell elements instead of 3D solid elements, can be adopted to analyze the steel– concrete composite plate girder up to the level of failure. The most appropriate properties of concrete in deck slab are simulated with this model and this model also predicts in a more appropriate way the behavior of a composite plate girder in the elastic as well as the plastic region.

To evaluate the contribution of the concrete slab to the shear resistance of composite concrete-steel plate girders, Sherafati *et al*. (2011) carried out two experimental tests. Their study was performed on one full-scale composite plate girder. The tested specimens were loaded to failure under shear load and positive moment. During the test, the vertical deflection of the girder and out-of-plane deflection of the web panels were monitored. The failure mechanism of the tested specimens was presented with the use of the test results. Nonlinear finite-element analysis of the tested specimen was performed with the use of the tests results. To study a larger group of composite girders, more finite-element models were made with different concrete slab and steel web thicknesses. The analytical and experimental results suggest a higher ultimate capacity of the tested composite specimen compared to what is predicted by the current AASHTO (2010) design specifications for a bare steel plate girder. A comprehensive model for considering the bond-slip effect in composite one-way slab section behavior has been proposed by Mousavi and Dehestani (2015). They have presented the procedure of considering bond-slip effects in finite-element numerical models. According to complex behavior of elements in composite sections, numerical modelling of composite sections is considered in many researches. In order to reduce the weight of long girders, various composite sections have been proposed in literature. Exodermic composite deck was studied experimentally and numerically by Allahyari *et al*. (2014). They used perfobond shear connectors in deck design. In a study by Alizadeh and Dehestani (2015), hybrid GFRP hat-shape sections were numerically considered. Hassanzadeh and Dehestani (2017) considered semi-confined composite beams. Confinement in their study was considered as the main subject.

1.1 Research significance

In this research, the composite beam under study includes metal beam and concrete slab which are connected by shear connectors welded to the metal beam. For the researchers of the field of structures, reduced beam height, which results in reduced beam weight, is always a great goal. Therefore, in this research, the section shape selected for the composite beam under study is trapezoidal, which has a lower height compared to other shapes with equal levels, and as a result, the beam weight is decreased. The internal metal beam space is completely empty and only for providing shear strength, at the two beam ends on the supports, the inside of the beam is covered with concrete, which also results in reduced consumed concrete volume and reduced beam weight. Also, a layer of concrete is covered on the metal beam. These two components, i.e. the concrete slab and the metal beam are connected to each other by grating shear connectors, and the bending strength of the composite beam, is highly affected by this connection method. Grating plates are used as shear connectors because a network of interconnected loops, results in higher confinement for the concrete. Furthermore, the hardness of the perforated plates is higher than spirals or channels made of round bars, and this type of plates will have a higher viscosity compared to plastic round bars.

In this study, because many research studies have been performed about composite beams consisting of concrete and steel, and models offered for this area, parameters influencing the bearing capacity of the composite beam have been investigated using a finite-element model. The accuracy of the finite-element model has been verified by comparing the results of the modelling with the results of laboratory tests (Fam and Honickman 2010), which are similar in terms of their section shape. In the following, the effect of some parameters such as steel trapezoidal section's dimensions' thickness, the thickness of concrete layer, and the thickness of confinement layer on the bearing capacity of structure will be evaluated and at the end; an optimal model will be designed for the beam section.

The main purpose of this research is to investigate the effect of the confinement degree parameters on the bearing capacity of steel concrete composite beam. The issue of confinement degree in the performance of composite beams subjected to displacement control loading has been of important and practical matters in this field, which has received little attention in research works. The provision of the above matters in a comprehensive way and also the comparison and investigation of the above parameters can offer a suitable view for the optimal design of composite beam section.

2. Finite element model

Finite element modeling is one of most useful methods for FRPs and reinforced concrete beams. It is capable for modeling and structural analysis of different aspects of a given structure such as material properties, element types as well as linear and non-linear behavior. Abaqus has been used as the preferred option for the current study.

2.1 Modeling of materials in Abaqus

Three different behavior models can be considered for concrete in the Abaqus materials library. However, the only model capable of solving reinforced concrete problems is the Concrete Damaged Plasticity (CDP) which is able to investigate reinforced concrete with different load bearings. It is also supplied with the strain-stress curves in tension

Table 1 Parameters in the plastic damage model for concrete

Poisson's ratio	Dilation Angle (degree)	Eeccentricity	σ_{b0}/σ_{c0}	k	Viscosity parameter
0.167	45	0.1	1.16	0.6667	0.001

Table 2 Properties of steel (St37)

Elastic	Steel's Elasticity module (GPa)	210
	Poisson's ratio	0.3
Plastic	First Yield stress (MPa)	370
	Second Yield stress (MPa)	520
	Plastic strain bending at First Yield Stress	0
	Plastic strain bending at second Yield Stress	0.21

and compression enabling it to consider the behavior of concrete more accurately. One of the advantageous features of this model is eliminating performance failures emerging in other programs. As a result, the authors have used CDP method to model 25 MPa concrete. Solid elements are generally used to model concrete in Abaqus and the common used element is 8 node 3D STRESS. The Abaqus elastic materials property library is applied for linear analysis in which Poisson ratio and elastic modulus are important. For complete description of the concrete behavior, not only these two parameters, but also the numerical values of five plastic parameters and specific parameters representing behavior of concrete in tension and compression are required. These parameters include dilation angle (φ), eccentricity (ε), which is the ratio of biaxial yield to uniaxial stress, (k) determining the shape of yield stress surface and finally viscosity (μ), representing relaxation time of the viscoplastic system. The values for these parameters are quantified in Table 1.

For simulations of the steel behavior, often the property of plastic behavior contained in Abaqus library is needed. In order to define steel materials Abaqus requires the user to supply one dimensional strain-stress curve as a function. However, for three-dimensional elements, the supplied strain-stress curve is used based on the Von Mises criterion. The linear analysis is then performed using embedded Abaqus elastic properties table.

In this study elastic modulus of steel, E=210 GPa and Poisson ratio is equal to 0.3. Similar to concrete elements, the eight node 3DSTRESS is also used for three-dimensional elements. Plastic properties are assigned to the elements for the purpose of steel element considerations, and the elastic property is used for the linear part of the strain–stress analysis.

There are also various models available in Abaqus for behaviors of studs; however, as the purpose of many designs and research in reinforced concrete is to idealize the behavior of steel, the compressive and tension behavior are

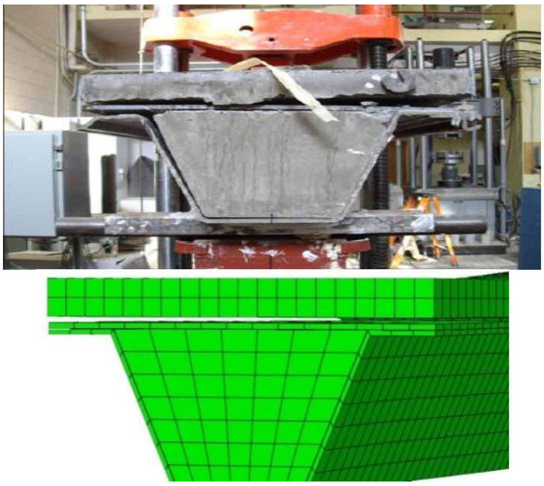

Fig. 1 Rupture in concrete and the GFRP layer in FEM (Fam and Honickman 2010)

assumed to be similar without affecting the final results. In order to reduce the time of the analysis and to avoid convergence problems in elastic-plastic models, the present study uses the isotropic bilinear elastoplastic models.

The definition of Young's modulus employs kinematic hardening, and the values entered into the software to support this definition are given in Table 2. In this method, the steel behaves elastically up to yield stress and then the slope, which is the hardening module of steel, continues up to the ultimate tensile strength.

Shell elements are employed for modeling steel studs. The effect of studs in the stiffness of concrete elements is used instead of modeling using independent elements by setting up an option called 'embedded" in the software. Studs are only interlocked with the surrounding concrete and the degrees of freedom of studs are equal to those of concrete. As studs are welded to the trapezoidal section, in reality, the finite-element model surrounding the studs is tied to the edges of trapezoidal section and the mesh density is designed not to exceed 50 mm for each cell.

The study further introduces composite beams and dedicates effects of parameters such as thickness and dimensions of trapezoidal section, confined length and deformation from trapezoidal to rectangular section on load bearing capacity and finally propose an optimal design for beam section. The problem of the effect of rate of confinement on performance of composite beams in controlled displacement loading is one of the important and applied topics, which has been rarely considered so far. These issues are well addressed in a comprehensive way, altogether with a parameter comparison, the paper hopes to reveal a better view for the optimal design of beam sections.

2.2 Validation of the finite element model

In order to validate the proposed model, the results have been compared to the experimental results by Fam and Honickman (2010), as in both studies the models are trapezoidal section and quasi-encased. The geometry of the beam is presented in Fig. 1. To evaluate the model, controlled displacement loading results were compared with

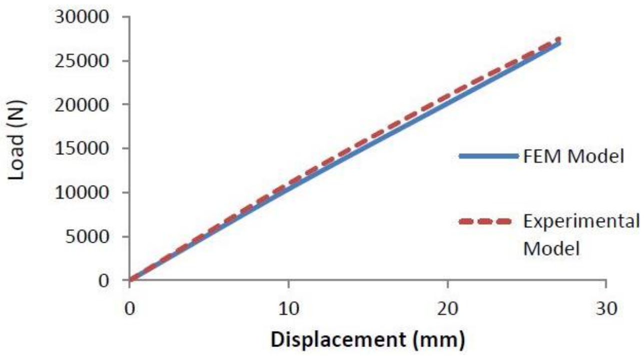

Fig. 2 Force-displacement diagram for experimental data (Fam and Honickman 2010) and FEM

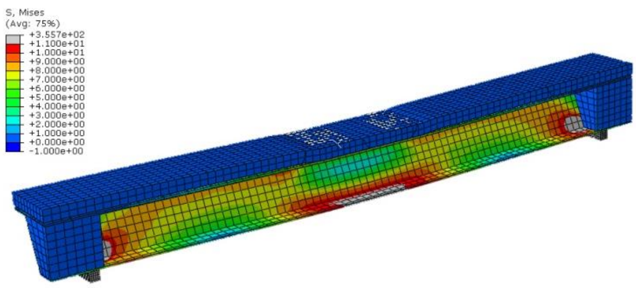

Fig. 3 Von-Mises stress contour plot

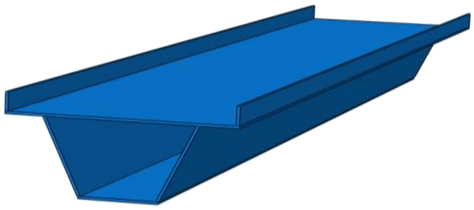

Fig. 4 Trapezoidal steel section

those from experiments. As it can be seen in Fig. 2, the force-displacement diagram linearly grows up to 276 kN and rapture will occur afterwards. However, in the experimental beam, 285 kN force applied on the beam can lead to 28 mm displacement, i.e., the yield value of the curve. Therefore, in the FE model, the load is applied in a controlled displacement manner (28 mm) in U2 direction so that the beam has already reached its load-bearing capacity of 278 kN. Fig. 2 compares experimental and FEM displacement-force diagrams. The result shows good agreement between FEM and experimental results in terms of formation and ultimate capacity. Fam and Honickman (2010) demonstrated that there is a detachment between concrete and GRFP layer; the same kind of detachment can be observed in FEM results shown in Fig. 2. Stress contour plot of the beam at the midsection plane is shown in Fig. 3 in order to better visualize the stress among inner sections of the GFRP.

3. Details of models and methodology

A brief introduction of the elements of a composite beam is given first. The investigated composite beam, which is shown in Fig. 4, is made of St37 steel and has a

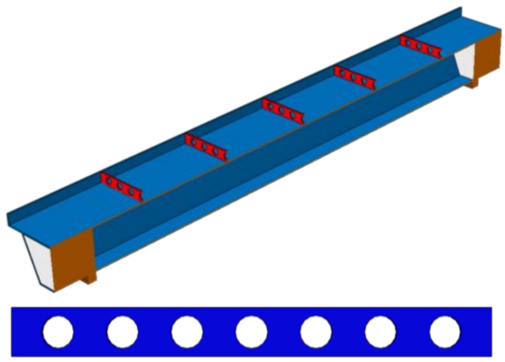

Fig. 5 Studs in FEM

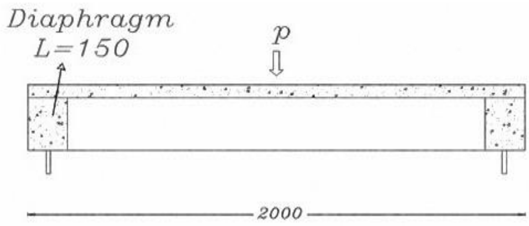

Fig. 6 Side face of beam M_1 and load point

trapezoidal section. It is preferred for its reduced height and also in turn reduced weight of the beam compared to the beams with rectangular shape sections. As shown in Figure 4 an extra knob like edge of the section can easily facilitate the confinement of the concrete. The advantage of this type of confinement is eliminating of the need for encasing (casting) for concrete, resulting in saved time and labor cost. A stud-reinforced concrete layer is placed on trapezoidal section as well as the two the ends of beam and the supports in order to increase the shearing resistance.

3.1 Studs (Perforated steel plates)

A mesh of connected rings has been long approved to have the most efficiency for the confinement of concrete. In this system, every ring is designed to locally confine a subtle piece of concrete, so that the whole concrete is confided. In this model, a perforated plate is used as the mesh is the system in such a way that every hole confines the concrete inside. These plates are easy to use and have a higher stiffness compared to ordinarily rebar meshes. On the other hand, these plates react against any tiny lateral concrete eformation and stop crack propagation and failure. Fig. 5 shows side view of the studs in FEM model.

The composite beam, which is called the primary beam M_1, is a ST and trapezoidal metal section with a thickness of 4 mm and height of 260 mm, which consists of a 200 mm height from the bottom to the edge to the and 60 mm in extra knob liked height that confines the concrete. The concrete layer has 60 mm thickness and compressive strength of 25 MPa. 4 mm steel studs are used to reinforce the concrete as mentioned in the last section. The span length of the beam is 2 m and two trapezoidal concrete pieces with 25 MPa compressive strength and 150 mm length are placed on the supports. The distance between the faces of supports to the edge of the beam is also 100 mm.

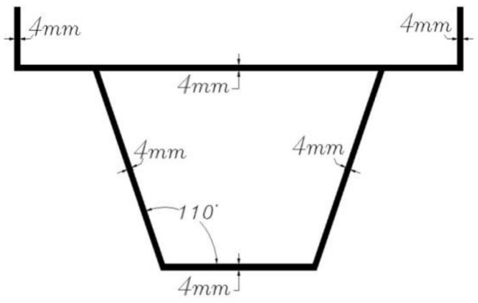

Fig. 7 Cross section of the primary beam M_1

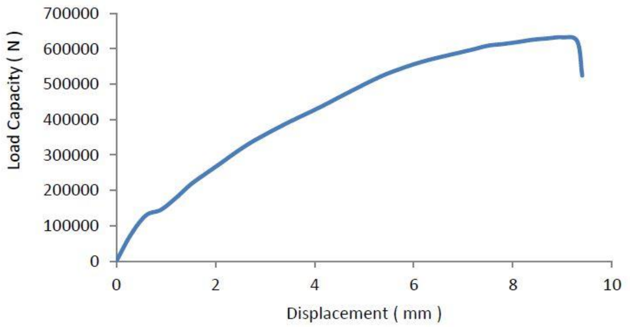

Fig. 8 Force displacement diagram of the beam of M_1

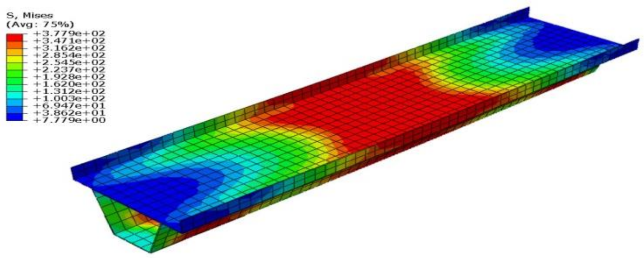

Fig. 9 Stress contour plot for the trapezoidal section of beam

Controlled displacement loading is applied on a 20 mm×20 mm plate on the center of the beam and the supports are considered as simple. The side face of the beam is shown in Fig. 6.

4. Steel-concrete composite beam design

The primary aim of this section is to design a section in which both concrete and steel could reach 60% to 70% of their ultimate capacity simultaneously i.e., both of the materials should reach 60% to 70% of their capacity at the same step for normal to severe service loads. As shown in Fig. 7, the thickness of all dimensions of the steel section in M1 is 4 mm. After many trials and errors, the dimensions of the section of the beam are designed so that the height from the lower edge of the section to the upper edge of the concrete is 264 mm and the width is 480 mm.

After analyzing the M1 applying different loads the results will look like Fig. 8, which shows the force-displacement curve for the point under the load. As it can be seen the slope of the curve will tend to reach zero after the value of the force increases up to 630 kN. Further extension

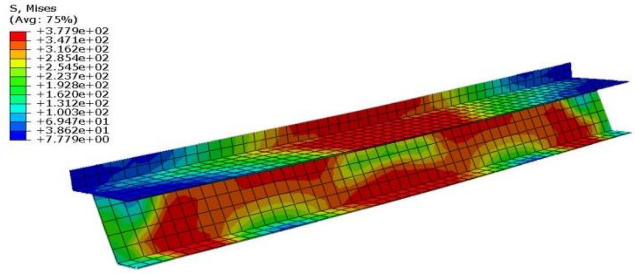

Fig. 10 Stress contour plot form inside of the trapezoidal section of beam

Table 3 Details of models

Finite element models	Thickness upper base T_e (mm)	web T_d (mm)	Thickness lower base T_b (mm)	Confinement thickness T_e (mm)	Confinement length L_e (mm)	Load bearing capacity (ton)
M_1	4	4	4	4	64	63
M_2	6	6	6	6	64	87
M_3	8	8	8	8	64	113
M_4	2.9	6	2.9	2.9	64	72.1
M_5	3.65	3.65	6	3.65	64	69.7
M_6	6	2.7	2.7	2.7	64	66.2
M_7	3.7	3.7	3.7	6	64	65.9
M_8	4.5	4.5	4.5	4.5	0	57
M_9	3.78	3.78	3.78	3.78	106.5	67
M_{10}	3.55	3.55	3.55	3.55	141	69

of the load can eventually lead the curve to a decline, which shows that it can no longer resist any more loads. This force is then considered as the ultimate capacity of the beam M1. It can also be seen that the rapture point of the structure is after the displacement reaches 9.0 mm and the load-bearing capacity is 630 kN. The Von-Mises stress Contour plot elements of the M1 are shown in Figs. 9 and 10.

In order to study the effects of various parameters on ultimate bearing load capacity several models with typical configurations of Fig. 11 were constructed. The details of the dimensions used in models are given in Table 3.

4.1 Effect of the section thickness on load bearing capacity

In this section, the effects of the thickness of different elements of the beam and confinement length are further studied more in order to give a new outlook to the reader. The first studied parameter as shown in Fig. 11 is the thickness of different dimensions of a trapezoidal steel section of the beam, as most of the conventional metals available commonly have thickness equal to 4 mm, 6 mm and 8 mm, the load-bearing capacity is investigated for these three different thicknesses.

In the second case, M_2, while retaining thickness and dimension of the first case unchanged, the thickness of the trapezoidal steel section is increased from 4 mm to 6 mm. The length "L_e" is the sum of concrete and the trapezoidal section thicknesses and equal to 66 mm. As a result of these modifications, the load-bearing capacity increased from 630 to 870 kN. The stress contour plot for the stud is shown in

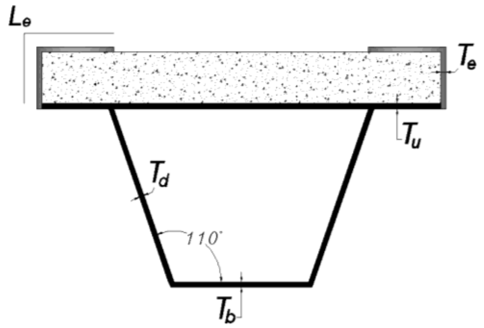

Fig. 11 Typical models configuration

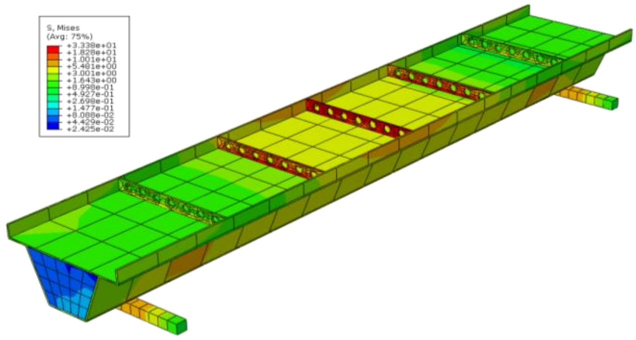

Fig. 14 stress contour plot for M_3

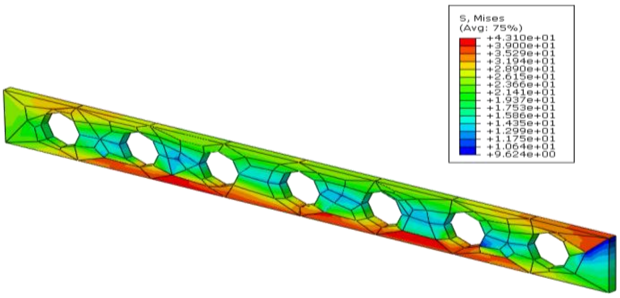

Fig. 12 Stress contour plot for stud (M_2)

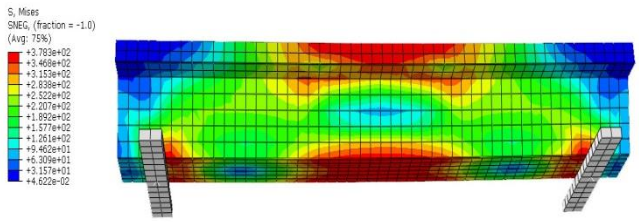

Fig. 15 Stress contour plot for M_4 beam

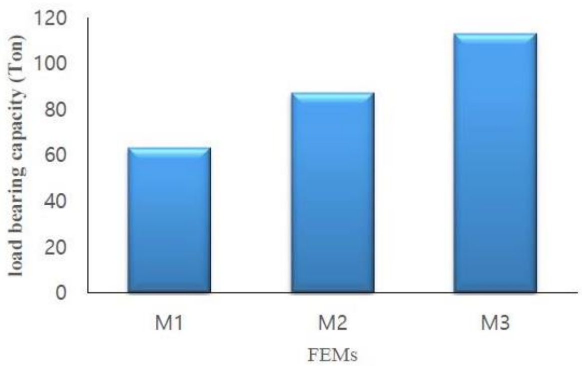

Fig. 13 Comparison of the load bearing capacities for M_1, M_2, M_3

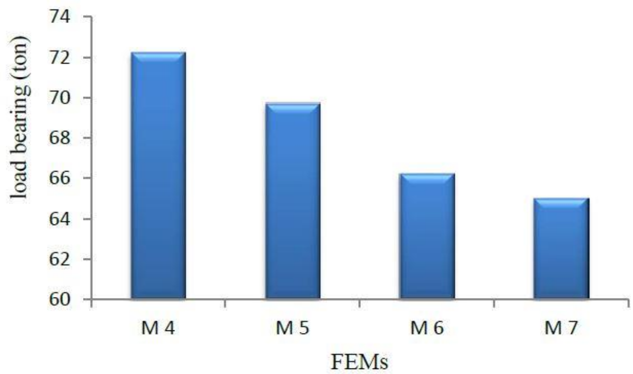

Fig. 16 Load bearing capacity for different thicknesses of the trapezoidal section

Fig. 12.

In the third case (M_3), the trapezoidal section thickness is changed from 4 mm to 8 mm and it has resulted in an increased load bearing capacity of 1130 kN.

The load bearing capacity for the three different cases investigated in this study M_1, M_2, M_3 are compared in Fig. 13 and the displacement contour for the model M_3 is shown in Fig. 14.

The next studied parameter is the thickness of the trapezoidal section in different dimensions. The method is to study the effect of a unique parameter on the bearing capacity of the main composite beam (M_1) by keeping all the other parameters as constant and at the same time changing the mentioned parameter to the desired value. Since the lengths of the different sides of the trapezoidal section are different, therefore we decrease the other lengths proportional to the increase in the unique length in order to keep the cross section area constant. In the M_4 model the effect of the web of the section (T_d) on the bearing capacity is studied by increasing it from 4 mm to 6 mm, while the other lengths are decreased to 2.9 mm to maintain the initial area of the section as constant. The results show that the bearing capacity increases up to 72 tf, 14% more than the initial bearing capacity of 63 tf. The stress contour plot for this section is shown in Fig. 15.

In the next case, M_5, the effect of the lower base of the section T_b is investigated by increasing the thickness from 4 mm to 6 mm while the other thickness has changed to 3.65 mm. This modification itself causes the initial 63 tf capacity to reach as high as 69.7 tf, showing around 10% increase.

In M_6 case the effect of upper base T_u is studied. Like the previous cases, as thickness of upper base change from 4 mm to 6 mm, the other dimensions will decrease to 2.7 mm, causing a 5% increase in load bearing capacity from initial 63 tf to 66 tf. In case M_7, the effect of the confining layer is examined thoroughly by increasing the 4 mm thickness to 6 mm that will increase the initial bearing capacity to 65.9 tf, while the other thicknesses are decreased from 4 mm to 3.7 mm.

Comparing the results shows that the web thickness (T_d)

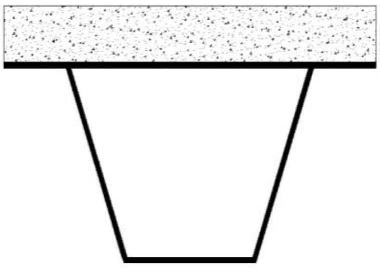

Fig. 17 M_8 cross section

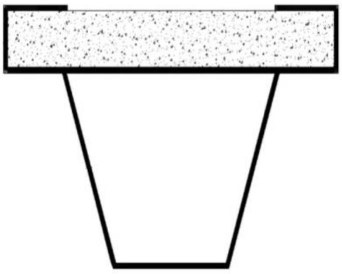

Fig. 18 M_9 cross section

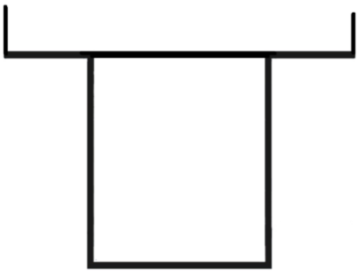

Fig. 19 Rectangular section of the beam

is the most effective parameter on the load-bearing capacity among all trapezoidal section side thicknesses. Fig. 16 compares the results for four different cases studied in this section.

4.2 Effect of confinement length (L_e) on composite beam bearing capacity

Considering M_1 as the base model, three different cases are studied for the effect of confinement length. In M_8, loading is carried without considering the confinement length in the calculations. In fact, we can let L_e=0 by keeping the other cross section thicknesses constant. This will change the bearing capacity from 63 tf to 57 tf, i.e., decreasing the confinement length to the edge of concrete will reduce the load-bearing capacity by 10%. The cross-section of M_8 is shown in Fig. 17.

As shown in Fig. 18, in the M_9 case the confinement length is set to reach half the length of lateral side of section, i.e., L_e=106 mm. For the initial area to remain constant, thickness of all other sides is decreased to 9 mm, these changes rise the capacity from 63 tf to 67 tf. For the case M_{10}, as shown in Fig. 18, the confinement length is increased up to the length of the lateral side of section resulting in an increase in capacity of the beam from 63 tf to 69 tf.

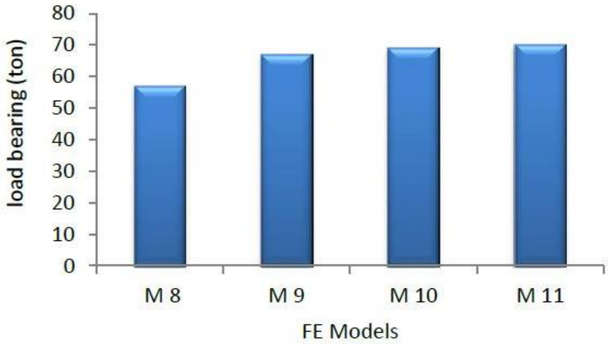

Fig. 20 Load bearing capacity for different lengths Confinement

4.3 Effect of changing cross section to rectangular shape

As the last step, another case (M_{11}) is investigated to compare the effect of changing the trapezoidal cross-section of M_1 to a quasi-encased rectangular one by keeping thickness values as before, in fact, the web of the section will change into vertical sides resulting in increased height from 200 mm to 212 mm and increased load bearing capacity from 63 tf to 70.1 tf. Although this parameter boost s the load-bearing capacity of the composite beam, given the fact that it increases the height of the section as well, it is not considered a useful way for optimization of the section of the beam. Fig. 19 shows the rectangular cross-section of the beam, and Fig. 20 compares the effect of parameters studied in this section on the load-bearing capacity.

5. An optimal composite beam design

Employing of the FEM software is proved to be accurate comparing to other experimental results reporting the load-bearing capacity of composite beams, nine different parameters such as trapezoid section thickness and length of confinement are then studied for the effect on the load-bearing capacity of the composite beam as illustrated and discussed earlier. The web thickness of the section is found to be the most effective parameter on the load-bearing capacity. Although changing the trapezoidal section to a rectangular shape results in an increase in the load-bearing capacity, given that the higher volume of concrete should be used and the higher weight of the beam requires the end supports to be changed making it an undesirable parameter for the optimal design of the beam.

Indeed, the purpose of optimization is to finally reach a more desirable capacity while the initial amount of materials remains unchanged. As mentioned before, the current study suggests that web thickness is the most effective parameter whereas the confining layer thickness is the least effective parameter on the beam load bearing capacity. So in order to have an optimized beam, in the main case M_1, while the thickness of the lower base T_b and the upper base T_u is kept constant, as confining layer decreases, the same value is added to web so that the

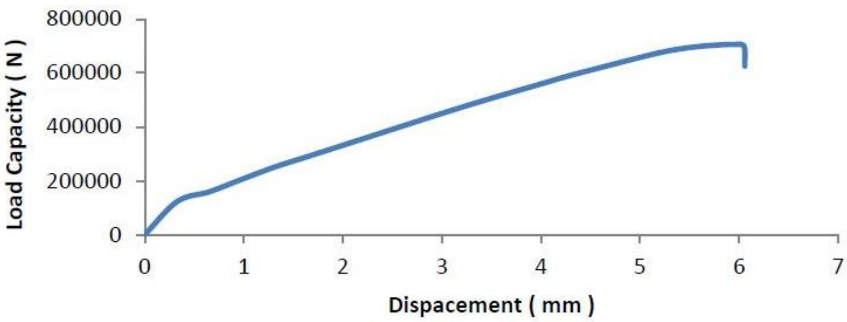

Fig. 21 Force displacement diagram of the optimized beam

amount of the material remains constant as well. These changes will therefore decrease the 4 mm confining layer length to 2 mm as web thickness rise from 4 mm to 4.7 mm. The load-bearing capacity will also increase from 63 tf to 70.8 tf accordingly. The force-displacement diagram for an optimized beam is sketched in Fig. 21.

6. Conclusions

In this research, the composite beam section under study includes a quasi-encased trapezoidal section of steel covered with a layer of concrete. Of the advantages of this confinement type to name is the lack of the need for concrete molding, which results in shorter concrete construction time, less cost and human resources. A layer of concrete reinforced with shear connector (perforated sheet) is placed on the trapezoidal steel section.

Initially, parameters affecting the bending performance and behavior of the quasi-encased composite beam have been investigated. Of these parameters to mention are the effects of the upper and lower bases thickness and the web thickness of the trapezoidal steel section, the effect of the thickness of the concrete layer, the effect of the section deformation from trapezoid to rectangle, the effect of the thickness and length of the confining layer on the beam’s bearing capacity.

The first parameter under investigation is the thickness of the trapezoidal section’s dimensions. By changing a parameter with a certain proportion and maintaining other parameters, the effect of it on the main composite beam’s bearing capacity called M_1 has been investigated. Since the trapezoidal section’s edges’ lengths were different, then in any state, the thickness is added by a factor that the other edges are decreased by the same factor that an edge’s section has been increased, so this way, the value of the new area will equal the primary cross section. By investigating the results from applying some changes, it’s concluded that the web thickness parameter (T_d) is introduced as the most effective parameter among the parameters of the thickness of the edges of the trapezoidal section. As a result, in this state, the beam’s shear performance is more important than its bending performance. Next, the parameter of confinement length has been investigated. In fact, the side edges of the trapezoidal section were stretched over to the concrete layer which prevents the separation of the concrete layer located on the trapezoidal steel section and results in the increase of the concrete’s bearing capacity. Although the bearing capacity of the beam increases by the deformation of the section from trapezoidal to rectangular, but since the deformation from trapezoidal to rectangular increases the section’s height, then it increases the beam’s weight and is not considered an optimal parameter for optimization.

In the next stage, by using the results obtained from investigating the parameters affecting the composite beam’s bearing capacity, the beam will be optimized, it means that a higher bearing capacity with the same amount of raw materials will be obtained such that when the concrete reaches the 60% to 70% of its bearing capacity, the steel will reach the same bearing capacity. As was investigated, among the effective parameters, the beam’s web thickness had the highest effect and the thickness of the confining layer, had the least effect on the increase of the beam’s bearing capacity, as a result, to optimize the section, in the main model M_1, by maintaining the thicknesses of the lower base T_b and upper base T_u, it was tried to decrease the thickness of the confining layer T_e and increase the web thickness T_d with the same value, so the materials volume would remain constant. Finally, by applying these changes, the structure’s bearing capacity increases from 63 t_f in the primary state of M_1 to 70.8 in the optimal state. In this investigation, various parameters such as number of studs, number of stud holes, studs thickness were investigated and were omitted from the text since they were not effective on bearing capacity of the composite beam.

Acknowledgments

Authors would like to appreciate the academic staff of the Faculty of Civil Engineering in Babol Noshirvani University of Technology of Iran, who kindly examined the research and suggested useful comments and modifications.

References

AASHTO LRFD (1983), Bridge Design Specifications, Washington DC, American Association of State Highway and Transportation Officials.

AASHTO LRFD (2010), Bridge Design Specifications, Washington DC, American Association of State Highway and Transportation Officials.

Abaqus, V. (2010), 6.10, User Subroutines Reference Manual.

Alghamdi, S.A. (2003), “Design optimization of non-uniform stiffened steel plate girders-A computer code", *Adv. Eng Softw*., **34**, 357-386.

Alizadeh, E. and Dehestani, M. (2015), "Analysis of composite girders with hybrid GFRP hat-shape sections and concrete slab", *Struct.Eng.Mech*. **54**(6), 1135-1152.

Allahyari, H., Dehestani, M., Beygi, M.H., Neya, B.N. and Rahmani, E. (2014), "Mechanical behavior of steel-concrete composite decks with perfobond shear connectors", *Steel Compos. Struct*., **7**(3), 339-358.

Ayoub, A. and Filippou, F.C. (2000), "Mixed formulation of nonlinear steel_concrete composite beam element", *J. Struct. Eng*., ASCE, **126**(3), 371-381.

Baskar, K., Shanmugam, N. and Thevendran, V. (2002), "Finite-element analysis of steel-concrete composite plate girder", *J. Struct. Eng*., **128**, 1158-1168.

Chacón, R., Mirambell, E. and Real, E. (2013), "Transver sally stiffened plate girders subjected to patch loading, Part 1, Preliminary study", *J. Constr. Steel Res*., **80**, 483-491.

Chapman, J.C. and Balakrishnan, S. (1964), "Experiments on composite beams", *Struct. Eng*., **42**, 369-383.

Darehshouri, S., Shanmugam, N. and Osman, S, (2013), "Ananalytical method for ultimate shear strength of composite plate girders with web openings", *Eng. Struct*., **56**, 610-620.

Della Corte, G., D'Aniello, M. and Landolfo, R. (2013), "Analytical and numerical study of plastic overstrength of shear links", *J. Constr. Steel Res.*, **82**, 19-32.

Fam, A. and Honickman, H. (2010), "Built-up hybrid composite box girders fabricated and tested in flexure", *Eng. Struct.*, **32**(4), 1028-1037.

Fukumoto, Y. and Nishida, S. (1981) "Ultimate load behaviour of curved I beams", *J. Eng. Mech. Div*., ASCE, **107**, 367-385.

Hassanzadeh, A.M. and Dehestani, M. (2017), "Numerical modeling of semi-confined composite beams consisting of GFRP and concrete", *Struct. Eng Mech*., **62**(1), 79-84.

Heins, C.P. and Fan, H.M. (1976), "Effective composite beam width at ultimate load", *J. Struct. Div*., ASCE, **102**(11), 2163-2179.

Heins, C.P. and Spates, K.R. (1970), "Behaviour of single horizontally curved girder", *J. Struct. Eng*., ASCE, **96**, 1511-1523.

Hendawi, S. and Frangopol, D.M. (1994), "Design of composite hybrid plate girder bridges based on reliability and optimization", *Struct. Saf.*, **15**, 149-165.

Hendy, C.R. and Turco, E. (2008), "Numerical valid ationof simplified theories for design rules of transversely stiffened plate girders", *Struct. Eng*., 37-42.

Kim, S.H., Choi, K.T., Park, S.J., Park, S.M. and Jung, C.Y. (2013), "Experimental shear resistance evaluation of Y-type perfobond rib shear connector", *J. Constr. Steel Res*., **82**, 1-18.

Kim, S.H., Park, S., Kim, K.S. and Jung, C.Y. (2017), "Generalized formulation for shear resistance on Y-type perfobond rib shear connectors", *J. Constr. Steel Res*., **128**, 245-260.

Kyung, K., Park, J., Jun, S. and Kim, J. (2011), "A study of the evaluation of fatigue crack at welded joint for steel plate girder", *Procedia Eng.*, **14**, 1543-1548.

Lee, H., Joo, H., Choi, B. and Moon, J. (2011), "Evaluation of flexural ductility of negative moment region of I-girder with high strength steel", *Procedia Eng*., **14**, 272-279.

LRFD (1994), A Manual of Steel Construction, American Institute of Steel Construction, Chicago.

Manfredi, G., Fabbrocino, G. and Cosenza, E. (1999), "Modeling of steel_concrete composite beams under negative bending", *J. Struct. Eng*., ASCE, **125**(6), 654-562.

Mattock, A.H.and Fountain, R.S. (1967), "Criteria for design of steel_concrete composite box girder highway bridge, Pittsburgh", United States Steel Corporation.

Mousavi, S.S. and Dehestani, M. (2015), "Implementation of bond-slip effects on behaviour of slabs in structures", *Comput. Concrete*, **16**(2), 311-327.

Nakai, H. and Yoo, C.H. (1988), *Analysis and Design of Curved Steel Bridges In New York*, McGraw-Hill.

Nakamura, S. (2002), "Bending behavior of composite girders with cold formed steel U section", *J. Struct. Eng*., ASCE, **128**(9), 1169-76.

Schelling, D.R., Galdos, N.H. and Sahin, M.A. (1992), "Evaluation of impact factors for horizontally curved steel box bridges", *J. Struct. Eng*., ASCE, **118**(1), 3203-3221.

Sennah, K.M. and Kennedy, J.B. (1999), "Load distribution factors for composite multicell box girder bridges", *J. Bridge Eng*., ASCE, **4**(1), 71-78.

Sennah, K.M., Zhang, X.S. and Kennedy, J.B. (2004), "Impact factors for horizontally curved composite box girder bridges", *J. Bridge Eng*., ASCE, **9**(6), 512-520.

Shanmugam, N.E., Lian, V.T. and Thevendran, V. (2002), "Finite Element Modeling of Plate Girders With Web Openings", *Thin Wall. Struct*., **40**, 443-464.

Sherafati, A., Farimani, R. and Azizinamini, A. (2011), "Effect of concrete slab on shear capacity of composite plate girders under positive moment", *J. Bridge Eng*., **18**, 89-98.

Slutter, R.G. and Driscoll, G.C. (1965), "Flexural strength of steel concrete composite beams", *J. Struct. Div*., ASCE, **91**(2), 71-99.

Thevendran, V., Shanmugam, N.E., Chen, S. and Liew, J.Y.R. (2000), "Experimental Study on steel_concrete composite beams curved in plan", *Eng. Struct*., **22**, 877-889.

Yam, L.C.P. and Chapman, J.C. (1968), "The inelastic behaviour of simply supported beam of steel and concrete", *J. Inst. Civil Eng*., **41**, 651-683.

CC